Eur. Phys. J. D **12**, 323–327 (2000)

THE EUROPEAN PHYSICAL JOURNAL D

EDP Sciences

Hydrogenated carbon clusters produced by highly charged ion impact on solid C_{84}

T. Schlathölter[1,a], M.W. Newman[2], T.R. Niedermayr[2], G.A. Machicoane[2], J.W. McDonald[2], T. Schenkel[2], R. Hoekstra[1], and A.V. Hamza[2]

[1] KVI Atomic Physics, Rijksuniversiteit Groningen, Zernikelaan 25, 9747AA Groningen, The Netherlands
[2] Lawrence Livermore National Laboratory, Livermore, California 94550, USA

Received 4 February 2000

Abstract. The emission of small (hydrogenated) carbon cluster ions $C_nH_m^+$ ($n = 2$–22) upon highly charged Xe^{q+} ($q = 20$–44) impact on C_{84} surfaces is studied by means of time-of-flight secondary ion mass spectrometry. The respective stage of hydrogenation/protonation of a certain carbon cluster ion C_n^+ is a strong indication for its geometrical structure. From the cluster ion yield as a function of cluster size it can be concluded, that the hydrogenation takes place after the initial carbon cluster formation. The carbon clusters seem to be emitted as an entity in agreement with "equilibrium" and "shock wave" models.

PACS. 36.40.Jn Reactivity of clusters – 61.48.+c Fullerenes and fullerene-related materials – 79.20.Rf Atomic, molecular, and ion beam impact and interactions with surfaces

1 Introduction

Exposition of a solid surface to energetic (keV) ions leads to the ejection of particles from the topmost layers. The so called sputtering process depends strongly on the type of the projectile ion. Singly charged atomic projectiles are commonly used for surface preparation. Mass spectrometry of charged sputtered particles (secondary ion mass spectrometry, SIMS) is a standard tool for surface analysis [1]. In a typical SIMS experiment the sputtered flux consists of (neutral and ionic) constituents of the surface, *i.e.* atoms and small molecules. However, even singly charged projectiles can eject larger entities from *e.g.* graphite surfaces, such as C_n^+ cluster ions with $n_{\max} \approx 30$ [2]. Unfortunately most of the sputtered material is neutral. Postionization is experimentally difficult and leads to additional excitation of the sputtered clusters which might alter the initial mass distribution. It is therefore straightforward to use projectiles which lead to a higher secondary ion yield, *e.g.* multiply charged projectiles [3]. Three possibilities which recently have been employed to sputtering of C_n^+ clusters from surfaces are impact of polyatomic projectiles on graphite and organic samples [4], MeV projectiles on polymer surfaces [5] as well as slow highly charged ions (HCI) on various surfaces [6]. In the latter study, Xe^{44+} was used to bombard *e.g.* a C_{84} target. In that case, the sputtered ion mass spectra extended to more than 200 C units. The yield of (small) cluster ions of size n followed a power law distribution $Y(n) \propto n^{-\tau}$, indicating the emission of clusters as an entity rather than cluster formation from independently excited atoms. It was concluded that the mass distribution depends strongly on the lifetime of a localized HCI induced excitation of a small near–surface volume.

However, the clusters were detected after only about 1 μs – an intermediate time for cluster fragmentation processes. Furthermore, the resolution of the study was limited to the separation of C_n^+ clusters, *i.e.* the influence of hydrogen present at the surface could not be studied. This paper should shed some light on formation as well as hydrogenation/protonation of C_n^+ ($n \leq 22$) clusters sputtered from a C_{84} target, continuing the studies mentioned above [6]. The obtained reactivity of the small carbon clusters will be compared to results obtained in gas-phase experiments, in particular to obtain information on electronic and geometrical cluster structure.

2 Experiment

Highly charged Xe ions were extracted from the Electron Beam Ion Trap (EBIT) at Lawrence Livermore National Laboratory [7], and reached the target chamber after momentum analysis in a 90° bending magnet. The extraction potential was set to 7 kV and projectiles of different charge states, q, reached the scattering chamber with kinetic energies of $7q$ keV. The influence of the kinetic energy on the emission of secondary ions following the impact of highly charged projectiles has been found to be small in the energy range of several hundred keV [8]. The pressure in the scattering chamber was kept at about 5×10^{-9} torr

[a] e-mail: tschlat@kvi.nl

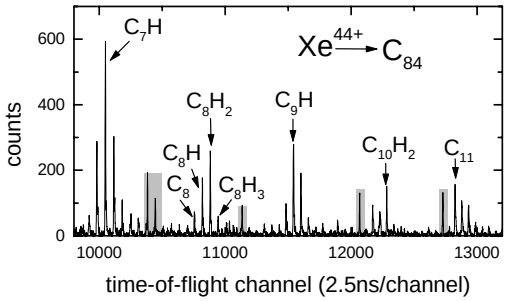

Fig. 1. C_7H_m–$C_{11}H_m$ part of a TOF-SIMS spectra for 211 keV Xe^{44+} projectiles impinging on solid C_{84}. For the C_7 and C_9 based clusters (odd n), the singly hydrogenated complex is most prominent, for C_8 and C_{10} based clusters (n even) it is the doubly hydrogenated one. From $n = 11$ on, the pure carbon cluster becomes strongest.

during analysis. Projectiles were decelerated by a target bias of +2.2 kV and impinged on the target with an incident angle of 45°. The beam spot had a diameter of about 1 mm. Positive secondary ions were extracted into a reflectron type time-of-flight secondary ion mass spectrometer. Details of the experimental setup have been described in reference [9]. The mass resolution of the spectrometer, $m/\Delta m$, was about 900 at 120 amu. The highly charged ion intensity was typically 1000 ions/s and time-of-flight cycles were started by protons that were emitted following the impact of individual projectiles. The start efficiency for protons is ≈50% for Xe^{44+}. If no proton is detected following the impact of a highly charged projectile, then a time-of-flight cycle may be started by heavier secondary ions such as H_2^+, H_3^+, etc. Flight times of secondary ions detected following non-proton starts ("false starts") are shifted relative to the dominant features of proton started spectra and are easily identified with time to mass calibration of the proton started features.

As target we used a micron-thick C_{84} layer, vacuum deposited on a Si(100) wafer. Prawer *et al.* [10] studied the damage of C_{60} films as a function of 620 keV Xe^+ exposure using *e.g.* Raman spectroscopy and atomic force microscopy. They found considerable destruction of the fullerene due to nuclear stopping for doses higher than $10^{11}/cm^2$. In our flux regime, we therefore expect degradation of the film only after several days of exposure. However, the ordering of the C_{60} film is distorted at much lower doses. Surprisingly, the ion beam radiation damage of thin fullerene films is due to nuclear rather than electronic energy transfer [11].

3 Results and discussion

Figure 1 shows a part of a m/q spectrum of sputtered clusters for 211 keV Xe^{44+} impact on a C_{84} surface. It is obvious, that for each base carbon cluster (C_7 to C_{11}) a multiplet of peaks is found. Besides the bare carbon clusters also species with one to three additional H atoms are prominent. Formation of hydrocarbon clusters has also been observed in MeV ion collisions with fullerene films [12]. The hydrogen originates most probably from surface contamination but also bulk contamination during film growth cannot be ruled out. The relative intensities of the C_n^+ and the $C_nH_m^+$ respectively depend strongly on the number of carbon atoms n. For $n = 7$ the C_7H^+ peak is strongest, *i.e.* formation of the monohydro product is preferred. The same holds for C_9^+. In case of the C_8^+ and C_{10}^+ clusters the dihydro products $C_8H_2^+$ and $C_{10}H_2^+$ are dominant. C_{11}^+ is most abundant in its bare form. In all cases the trihydro species are already relatively weak and clusters containing more than three hydrogen atoms have negligible intensity.

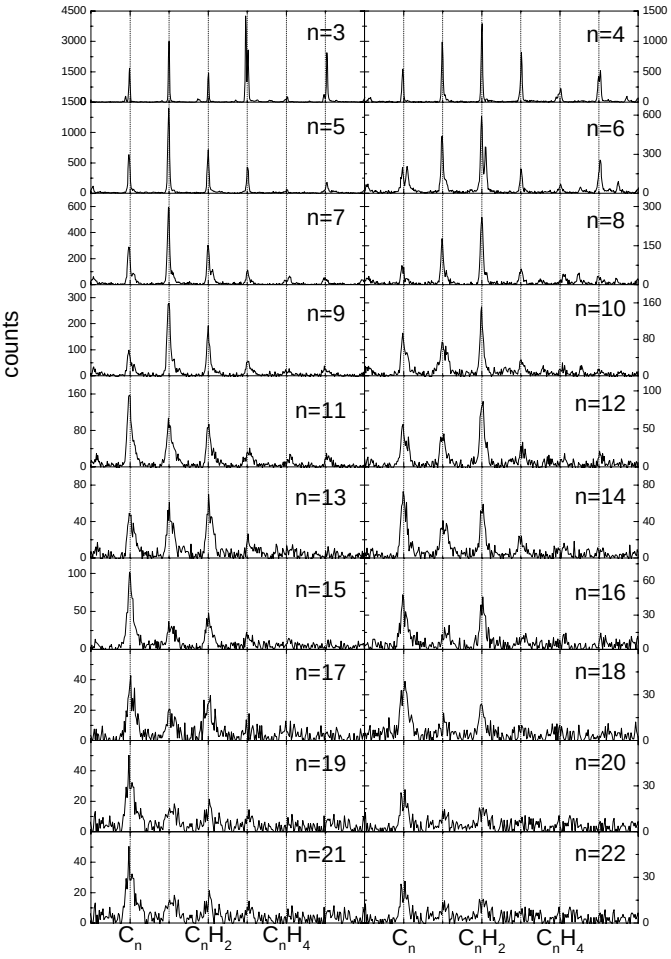

Fig. 2. m/q spectra for the same data as in Figure 1. The peaks for all relevant C_nH_m clusters for n =3–22 are shown with separate plots for each n. Each plot ranges from mass number $12n - 1$ to $12n + 6$.

The peaks shaded grey do not follow the systematic size dependence of the hydrocarbon clusters. Most probably, these peaks are due to contaminants on the surface which stem from the target handling.

The overall pattern can be studied in the m/q spectra of Figure 2. The data shown are from the same spectrum as in Figure 1. A different behaviour is found for odd and even n respectively. In case of odd n values ($n \leq 10$) the monohydro species (C_nH^+) is always the most prominent

peak being relatively strongest for $n = 9$. For even n values ($n \leq 12$) on the other hand the dihydro product is strongest. The $n = 11$ cluster family is the first with completely different peak ratios, the bare C_{11}^+ is by far the strongest structure. The same holds for $n = 15$. With this exception, all clusters (even and odd) show a similar behaviour for $n > 12$. The relative yield of bare C_n^+ is the highest and it increases with n. The dihydro species yield always exceeds the one of monohydro species.

To interpret these findings it is helpful to first summarize some recent findings on the geometrical and electronic structure of carbon clusters.

From theoretical studies it is known, that (neutral and positively charged) carbon clusters all possess low-energy linear geometries for $n < 10$ [13]. For even n, also cyclic isomers are possible and seem to be even slightly lower in energy. Nevertheless, these geometries are less abundant because of their much lower entropy, and therefore they are difficult to detect experimentally [13,14]. In case of $n = 10$ the cyclic isomer is about 1 eV more stable than the linear one, therefore this cluster represents a transition between linear and cyclic structures. Larger n values should always lead to cyclic structures. For the small linear clusters a cumulenic bonding structure (:C=C=C=C=C:) is expected. Judging from this, no difference in the reactivity regarding hydrogen should be observed. Reaction experiments involving gas phase carbon clusters and molecular hydrogen however indicate that the even numbered carbon clusters C_4, C_6 and C_8 (as well as the linear isomers for clusters with larger n) have a polyyne structure with alternating bonds (·C≡C–C≡C–C≡C·) [15]. H atom addition to both highly reactive ends of such a chain leads to C_nH_2 which is indeed the most prominent peak for $n \leq 10$ (n even) in Figure 2. The same was also found by Kroto *et al.* [15] for reactions of gas phase C_n with H_2 and H_2O, *i.e.* condensation of the C_n clusters in He-buffer gas contaminated with small amounts of H_2 or H_2O. For the odd clusters no polyyne bonding is possible so they have to possess the less reactive cumulene structure. Indeed we observe the C_nH^+ to be strongest for $n \leq 10$ (n odd).

It has to be noted, that a comparison of reactivities of neutral and ionic clusters can be critical. However, in cluster sputtering experiments the formation of the final charge state and the cluster conformation itself cannot be clearly separated.

The reactivity of larger carbon clusters ($n = 8$–37) during their formation phase has been studied experimentally by Hallett *et al.* [16]. The relative intensities of pure C_n and C_nH_m depend strongly on the hydrogen concentration in the buffer gas used during cluster vaporization from graphite. For low concentrations and even n, a clear dihydro contribution C_nH_2 is found exceeding the pure C_n peak. These findings are in some agreement with our results in the sense, that the dihydro species exceeds the $C_nH_m^+$ maxima. The fact that we observe the bare C_n^+ as strongest might be due to a lower amount of hydrogen available in our experiment. For the "magic" clusters C_{11}, C_{15} and C_{19} Hallett *et al.* find the bare carbon cluster to be most intensive. This is in agreement with our data

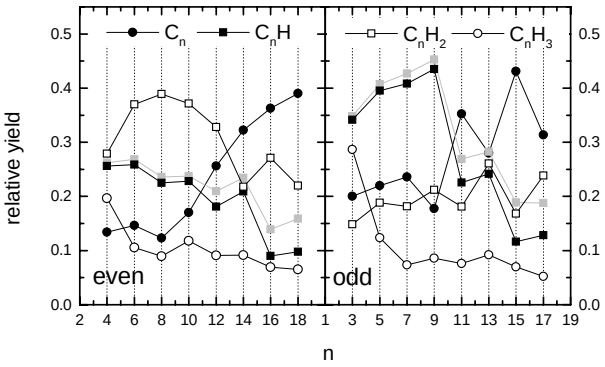

Fig. 3. Relative yields of C_n^+ (•), C_nH^+ (■), $C_nH_2^+$ (□) and $C_nH_3^+$ (○) as a function of the number of carbon atoms n. The integral of these four peaks is taken as reference.

(especially for $n = 11$, 15) and might be due to the high stability of the magic numbered clusters. On the other hand, our results regarding the $n = 13, 17$ clusters show no peculiar behaviour whereas Hallett *et al.* find these cluster families to be strongly suppressed. For the remaining odd values of n their results show substantial bare clusters with increasing importance of the monohydro species whereas we just observe a high bare cluster yield and weak monohydro and dihydro products over the whole range.

Figure 3 quantifies the statements from above. To obtain the relative values the integrals of all $C_nH_m^+$ ($n = 3$–20, $m = 0$–3) peaks have been calculated and divided by the sum of all four peaks ($m = 0$–3) for a given n. The evaluation is complicated by the 1.108% natural abundance of ^{13}C. For instance $^{12}C_nH$ cannot be separated from $^{12}C_{n-1}{}^{13}C$. With increasing n this effect becomes important and the data in Figure 3 have been corrected accordingly – as an example, for the singly hydrogenated species the raw data are plotted in light gray. For higher degrees of hydrogenization, the isotope effect has also been corrected.

From Figure 2 it is obvious that for a given n by far the most clusters contain less than four H atoms.

For even n and $n \leq 12$ $C_nH_2^+$ is dominant. Over the whole range it exceeds the monohydrogenated C_nH^+. The pure C_n^+ cluster intensity starts relatively low and increases monotonically for $n > 8$. The trihydrogenated species are weak over the whole range.

For odd n and $n < 11$ the C_nH^+ is relatively strongest. With increasing n the dihydro species becomes more important and is relatively stronger for $n > 11$. For low n the pure carbon cluster C_n is always exceeding the neighbouring values for even n (the usual even-odd oscillations observed in most mass spectra of small carbon clusters). For $n > 9$ the relative C_n^+ yield generally increases though not monotonically (because of the extremely high values for the magic numbers $n = 11$ and $n = 15$).

The similarity of gas phase and HCI induced sputtering experiments is not surprising since in our experiment energy deposition and cluster formation are largely decoupled. The (potential) energy deposition itself takes place

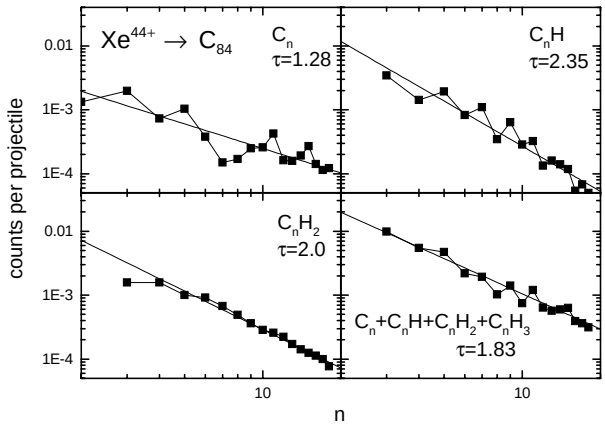

Fig. 4. Secondary ion counts per projectile of C_n, C_nH, C_nH_2 and $\sum_{m=0}^{3} C_nH_m$ ions as a function of carbon cluster size n for Xe^{44+} impact. The number of start signals (detected protons) is defined as unity. The solid lines are power-law fits with the exponent τ given on each plot.

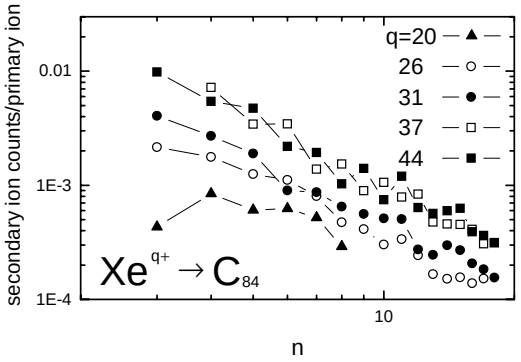

Fig. 5. Secondary ion counts per projectile of $\sum_{m=0}^{3} C_nH_m^+$ as a function of the carbon cluster size n for $7q$ keV Xe^{q+} impact ($q = 20$–44). The number of start signals (detected protons) is defined as unity.

on a 10 fs timescale (neutralization and deexcitation of the projectile above and within the first layer). Energy redistribution processes and the transfer from electronic excitation to kinetic energy of target constituents on the other hand occurs on typical vibrational timescales of 100 fs and several ps.

The absolute cluster yields for the $C_nH_m^+$ species are shown in Figure 4, again for 211 keV Xe^{44+} projectiles. The number of start signals is taken as a reference. It is obvious, that for all stages of hydrogenation the cluster yield decreases with n. The solid lines on the double-logarithmic plots are power-law fits $Y(n) \propto n^{-\tau}$ with τ indicated on each plot. The cluster size dependence of the bare carbon cluster shows an overall agreement with a power law ($\tau = 1.28 \pm 0.19$) but is dominated by even-odd oscillations and the strong magic numbers $n = 11, 15$. The monohydro species shows better agreement with a power-law fit ($\tau = 2.35 \pm 0.15$) but still even-odd oscillations are visible. As expected, no strong maxima corresponding to magic numbers are observed. For the dihydro species, the oscillations vanish and the fit is nearly perfect $\tau = 2.0 \pm 0.08$). The last figure shows the summed data which is described by a fit with $\tau = 1.83 \pm 0.09$.

It is a quite general phenomenon, that multifragmentation processes give rise to mass distributions following a power law with critical exponents around $\tau = 2$, *e.g.* in collisions of MeV ^{12}C with ^{108}Ag ($\tau = 2.18$) or collisions of two basalt spheres ($\tau = 1.68$) [17]. In [6] it was already shown for Xe^{44+} impact on a fullerene surface, that from the power-law dependence of the sputtered cluster yield the underlying mechanism can be concluded to be ablation of complete clusters rather than formation of clusters from sputtered atoms and molecules. Hamza *et al.* [18] found the same power law dependence in HCI induced sputtering of $(UO_x)_n^+$ clusters from UO_2 targets ($\tau \approx 2$). Apparently the sputtering process can be viewed as a fragmentation of the surface. Two models for the sputtering mechanism could be (i) the emission as entity model [19] in which the incoming ion causes a shock wave and clusters are ablated from the near-surface region subsequently and (ii) the cluster sputtering model [20] in which a small area of the surface is assumed to undergo liquid-gas phase transition due to the large amount of locally deposited energy. Both models lead to exponents around -2 and therefore it is impossible to decide which model is correct. A possible explanation for model (i) could be a Coulomb explosion due to the large amount of charge deposited into the surface on a short time-scale [21].

As mentioned above the $C_nH_m^+$ yields in Figure 4 do not exactly follow a power law with $\tau \approx 2$ for $m = 0$, 1 ($\tau = 1.28, 2.35$), whereas the total yields ($\tau = 1.83$) are close. Within the cluster sputtering models this can only be explained by a two step model: the hydrogenation takes place in a late stage of the desorption process after C_n cluster formation in the primary excitation process, *i.e.* for a given n all $C_nH_m^+$ clusters stem from the same C_n parent which may pick up hydrogen when leaving the surface. In this sense bare clusters are emitted as an entity. The hydrogen pickup is expected to be sensitive to cluster geometry, size and reactivity, which explains the good overall agreement with the gas phase experiments mentioned above.

The dependence of the cluster size distribution on the projectile charge state is shown in Figure 5 for Xe^{q+} impact on C_{84}.

It is obvious, that for all charge states (except $q = 20$ for which just small clusters are observed) a linear n dependence is observed in the double-logarithmic plot. In particular, the exponents n for $q = 26, 31, 37, 44$ are 1.85, 1.8, 2.05 and 1.83 respectively. Furthermore, an increase of the absolute yield with the projectile charge state q is observed. This increase is clearly due to the increased potential energy of the projectile (the kinetic energy of the projectile is expected to be negligible for HCI induced sputtering [7,8]) and has been found for several other collision systems.

An open question is whether the presented results are specific for a fullerene target. The fact, that we observe sputtered (or desorbed) fullerene ions between C_{84} and C_{60} (not shown in the figures) is certainly a unique feature of fullerene targets. For the low mass region the answer is more difficult. Gas phase collisions of C_{60}^+ with H_2 and He ($v \approx 0.1$ a.u. [22,23]) give rise to mass spectra of intermediate fragment C_n^+ cluster sizes with maxima at the magic numbers $n = 15$ and $n = 19$. Besides the C_{60}^{q+} with the respective evaporation series C_{60-2n}^{q+} an additional group of fullerenes is observed with $n \approx 44$. In our sputtering experiments, we observe a completely different small fragment distribution and find no indication for a fragmentation pattern around $n \approx 44$. On the other hand, in gas phase collisions of highly charged ions with fullerenes at $v \approx 0.2-0.4$ a.u. a bimodal distribution is observed, *i.e.* the maxima are found at $n = 1$ and $n = 60$ and no clusters of intermediate size ($n \approx 20-40$) are observed [24–27]. Projectiles with large potential energy can lead to an excitation of the fullerene which is sufficient to erase all structural information.

Based on that, it can be expected to observe emitted cluster distributions similar to those of C_{84} targets when sputtering graphite or maybe even diamond targets. Minor differences could be expected due to the different bonding of the carbon allotropes (graphite: sp^2, diamond: sp^3, fullerenes: sp^2 and sp^3).

4 Summary

The emission of C_n^+ clusters upon C_{84} film bombardment by slow Xe^{q+} ions is due to emission of entire clusters from the surface. Hydrogenization takes place as a final step during desorption, after the primary sputtering process. In this sense, we observe no full "emission as entity".

The degree of hydrogenization of a particular C_n^+ cluster allows a rough determination of its geometry. In accordance with gas phase experiments, for $n \leq 10$ cumulenic or polyyne bond linear clusters are most probable, whereas the larger clusters seem to be cyclic. The results of cluster sputtering and hydrogenization by HCI are very similar to the results of gas phase carbon cluster formation in hydrogen rich environments, suggesting that also for the system under study, the formation of positive hydrocarbon clusters is dominated by the chemical properties of carbon rather than by different primary excitation mechanism.

This work was performed under the auspices of the U.S. Department of Energy by Lawrence Livermore National Laboratory under contract No. W-7405-ENG-48. TS and RH gratefully acknowledge financial support from the Stichting voor Fundamenteel Onderzoek der Materie (FOM) which is supported by the Nederlandse Organisatie voor Wetenschapelijk Onderzoek (NWO).

References

1. A. Benninghoven, Surf. Sci. **299/300**, 246 (1994).
2. H. Gnaser, Nucl. Instrum. Meth. B **149**, 38 (1999).
3. S.T. deZwart, T. Fried, D.A. Boerma, R. Hoekstra, A.G. Drentje, A.L. Boers, Surf. Sci. **177**, L939 (1986).
4. K. Baudin, A. Brunelle, S. Della-Negra, D. Jacquet, P. Hakansson, Y. LeBeyec, M. Pautrat, R.R. Pinho, Ch. Schoppmann, Nucl. Instrum. Meth. B **112**, 59 (1996).
5. C.W. Diehnelt, M.J. van Stipdonk, E.A. Schweikert, Phys. Rev. A **59**, 4470 (1999).
6. T. Schenkel, A.V. Barnes, A.V. Hamza, D.H. Schneider, Eur. Phys. J. D **1**, 297 (1998).
7. T. Schenkel, A.V. Hamza, A.V. Barnes, D.H. Schneider, Prog. Surf. Sci. **61**, 23 (1999).
8. T. Schenkel, A.V. Barnes, M.A. Briere, A.V. Hamza, A. Schach von Wittenau, D.H. Schneider, Nucl. Instrum. Meth. B **125**, 153 (1997).
9. T. Schenkel, A.V. Hamza, A.V. Barnes, M.W. Newman, G. Machicoane, T. Niedermayer, M. Hattass, J.W. McDonald, D.H. Schneider, K.J. Wu, R.W. Odom, Phys. Scripta **T80**, 73 (1999).
10. S. Prawer, K.W. Nugent, S. Biggs, D.G. McCulloch, W.H. Leong, A. Hoffman, R. Kalish, Phys. Rev. B **52**, 841 (1995).
11. D. Fink, R. Klett, P. Szimkoviak, J. Kastner, L. Palmetshofer, L.T. Chadderton, L. Wang, H. Kuzmany, Nucl. Instrum. Meth. B **108**, 114 (1996).
12. R.N. Papaleo, P. Demirev, J. Eriksson, P. Hakansson, B.U.R. Sundqvist, Phys. Rev. B **54**, 3173 (1994).
13. A. van Orden, R. Saykally, Chem. Rev. **98**, 2313 (1998).
14. W. Weltner, R.J. van Zee, Chem. Rev. **89**, 1713 (1989).
15. H.W. Kroto, J.R. Heath, S.C. O'Brien, R.F. Curl, R.E. Smalley, Astrophys. J. **314**, 352 (1988).
16. R.P. Hallett, K.G. McKay, S.P. Balm, A.W. Allaf, H.W. Kroto, A.J. Stace, Z. Phys. D **34**, 65 (1995).
17. J. Hüfner, D. Mukhopadhyay, Phys. Lett. B **173**, 373 (1986).
18. A.V. Hamza, T. Schenkel, A.V. Barnes, Eur. Phys. J. D **6**, 83 (1999).
19. I.S. Bitensky, E.S. Parilis, Nucl. Instrum. Meth. B **21**, 26 (1987).
20. H.M. Urbassek, Rad. Eff. Def. Sol. **109**, 293 (1989).
21. I. S. Bitensky, M.N. Murakhmetov, E.S. Parilis, Soviet. Phys. Tech. Phys. **24**, 618 (1979).
22. P. Hvelplund, L.H. Andersen, H.K. Haugen, J. Lindhard, D.C. Lorents, R. Malhotra, R. Ruoff, Phys. Rev. Lett. **69**, 1915 (1992).
23. R. Vandenbosch, B.P. Henry, C. Cooper, M.L. Gardel, J.F. Liang, D.I. Will, Phys. Rev. Lett. **81**, 1821 (1998).
24. B. Walch, C.L. Cocke, R. Voelpel, E. Salzborn, Phys. Rev. Lett. **72**, 1439 (1994).
25. T. Schlathölter, R. Hoekstra, R. Morgenstern, J. Phys. B.: At. Mol. Opt. Phys. **31**, 1321 (1998).
26. H. Cederquist, A. Fardi, K. Haghighat, A. Langereis, H.T. Schmidt, S.H. Schwarz, J.C. Levin, I.A. Sellin, H. Lebius, B. Huber, M.O. Larsson, P. Hvelplund, Phys. Rev. A **61**, 022712 (2000).
27. S. Martin, L. Chen, A. Denis, S. Desesquelles, Phys. Rev. A **59**, R1734 (1999).